



ELSEVIER

Fluid Dynamics Research 28 (2001) 237–265

**FLUID DYNAMICS
RESEARCH**

Linear and nonlinear dynamo properties of time-dependent ABC flows

N.H. Brummell^{a,*}, F. Cattaneo^b, S.M. Tobias^{a,c}^a*JILA & Department of Astrophysical and Planetary Science, University of Colorado, Boulder, CO 80309, USA*^b*Department of Astronomy and Astrophysics, University of Chicago, Chicago, IL 60637, USA*^c*Present address: Department of Applied Mathematics, The University of Leeds, Leeds LS2 9JT, UK*

Accepted 9 August 2000

Abstract

The linear and nonlinear dynamo properties of a class of periodically forced flows is considered. The forcing functions are chosen to drive, in the absence of magnetic effects (kinematic regime), a time-dependent version of the ABC flow with $A = B = C = 1$. The time-dependence consists of a harmonic displacement of the origin along the line $x = y = z = 1$ with amplitude ε and frequency Ω . The finite-time Lyapunov exponents are computed for several values of ε and Ω . It is found that for values of these parameters near unity chaotic streamlines occupy most of the volume. In this parameter range, and for moderate kinetic and magnetic Reynolds numbers, the basic flow is both hydrodynamically and hydromagnetically unstable. However, the dynamo instability has a higher growth rate than the hydrodynamic one, so that the nonlinear regime can be reached with negligible departures from the basic ABC flow.

In the nonlinear regime, two distinct classes of behaviour are observed. In one, the exponential growth of the magnetic field saturates and the dynamo settles to a stationary state whereby the magnetic energy is maintained indefinitely. In the other the velocity field evolves to a nondynamo state and the magnetic field, following an initial amplification, decays to zero. The transition from the dynamo to the nondynamo state can be mediated by the hydrodynamic instability or by magnetic perturbations. The properties of the ensuing nonlinear dynamo states are investigated for different parameter values. The implications for a general theory of nonlinear dynamos are discussed. © 2001 Published by The Japan Society of Fluid Mechanics and Elsevier Science B.V. All rights reserved.

1. Introduction

Dynamo action describes the generation of magnetic fields within the bulk of a conducting fluid (Cowling, 1957; Moffatt, 1978). Dynamo processes are commonly invoked to explain the origin of magnetic fields in astrophysical systems such as planets, stars and galaxies (Parker, 1979; Zel'dovich et al., 1983). In order for dynamo processes to be physically meaningful, they should not only account

* Corresponding author.

E-mail address: brummell@solar.colorado.edu (N.H. Brummell).

for the amplification of magnetic fields from initial conditions of weak magnetization but also for the maintenance of such fields at the observed levels against the action of Ohmic dissipation. These two aspects of dynamo action, field amplification and field maintenance correspond to two distinct phases of the dynamo process, and from a mathematical point of view require somewhat different treatments.

The process of field amplification is traditionally discussed within the framework of *kinematic* dynamo theory. Physically, it is assumed that at some early epoch the magnetic field is sufficiently weak to be dynamically irrelevant. In this regime, the velocity of the fluid is determined by the externally imposed forces, and can itself be considered as prescribed once these driving forces are given. Under this assumption, the dynamo problem becomes *linear* and can be conveniently formulated in terms of an eigenvalue problem for the dynamo growth rate. The two central objectives of kinematic dynamo theory are then the identification of those properties of velocities that lead to dynamo action, and the description of the structure of the resulting magnetic field (Moffatt, 1978; Childress and Gilbert, 1995).

As the magnetic field grows, the corresponding magnetically induced forces also increase and eventually become, either locally or globally, comparable to the other terms in the momentum balance equation. These cause a modification of the underlying velocity field that ultimately leads to the saturation of the amplification process. In many cases, a dynamic balance is reached between driving and magnetic retarding forces and the dynamo system settles into a stationary state whereby the magnetic field is maintained at some finite-level indefinitely (Meneguzzi and Pouquet, 1989; Kida et al., 1991; Nordlund et al., 1992; Galanti et al., 1992; Seehafer et al., 1996; Brummell et al., 1998; Zienicke et al., 1998; Cattaneo, 1999; Fuchs et al., 1999). The mathematical treatment of the saturation process as well as the description of the resulting stationary state require that both the magnetic field and the velocity be calculated self-consistently. In other words, a fully nonlinear approach is needed. The simultaneous solution of the induction equation, describing the magnetic field evolution, and the momentum balance equation, describing the evolution of the velocity, present a problem of considerable complexity. As a result, quite a lot is known about the kinematic dynamo problem and relatively little about the nonlinear one.

The study of nonlinear dynamos often relies on the numerical solution of the magnetohydrodynamics (MHD) equations and has therefore flourished in recent years with the increase in computational resources. There are a number of challenges associated with such studies that deserve to be mentioned here. Dynamos are intrinsically three-dimensional, and in many cases the physically interesting regimes are defined by large kinetic and magnetic Reynolds numbers – i.e. small viscosity and magnetic diffusivity. This leads to heavy computational requirements if the nonlinear MHD state is to be accurately represented. Another problem is that it is often difficult to relate the kinematic and nonlinear regimes in a natural way. The kinematic problem is typically defined in terms of prescribed velocities, whereas the nonlinear problem must be defined in terms of prescribed external forces (Moffatt, 1972; Brummell et al., 1998). It can be argued that for any given velocity the momentum equation could be “inverted” to give the required forcing function to drive any desired velocity. However, more often than not, the candidate velocities for kinematic dynamo action are hydrodynamically unstable even at moderate kinetic Reynolds numbers (Zheligovsky and Pouquet, 1993). As a result, the velocity drifts away from the desired flow even in the kinematic regime.

A number of studies have partially circumvented these problems by resorting to various approximations that represent the magnetic back reaction in a simplified manner, and/or restrict the possible

ways in which the velocity field can be modified (Cattaneo et al., 1996). The advantages of these approaches is that they afford considerable savings in computational requirements, and can be used to relate the kinematic and nonlinear phases in a natural way. The main disadvantage is that lacking a deeper understanding of nonlinear dynamos in general, or a fully nonlinear model for comparison, it is difficult to assess how well they represent the physics of the saturation process.

In the present paper, we address some of these issues by means of well resolved, fully nonlinear simulations of the (incompressible) MHD equations. We are primarily concerned with the nonlinear regime, in particular the structure of the nonlinear dynamo states, and their dependence on the defining parameters. However, we also strive to retain some relationship between the nonlinear and kinematic regimes. To achieve this, we have chosen a family of velocities, and hence forcing functions that helps us circumvent some of the problems related to the hydrodynamic instability of the basic flows.

The remainder of this paper proceeds as follows. Section 2 contains the formulation of the problem and a brief outline of the numerical method of solution. Section 3 introduces the family of kinematic velocities used here and their Eulerian and Lagrangian properties. The solutions resulting from the chosen forcing in the kinematic regime are described in Section 4, with the nonlinear properties examined in Section 5. Section 6 further examines the interaction between hydrodynamic and magnetic instabilities and the surprising nonlinear behaviour that can result. Concluding remarks are contained in Section 7.

2. Formulation

Our objective is to study the transition between the kinematic and dynamic regimes and to examine the ensuing properties of fully nonlinear solutions. We consider dynamo action in an incompressible fluid with finite viscosity and electrical conductivity in a periodic domain with 2π periodicity in all three directions. The evolution of this system is described by the magnetic induction equation, the momentum balance (Navier–Stokes) equation, and the constraints that the magnetic and velocity fields be solenoidal, which we write here in dimensionless form:

$$(\partial_t - R_m^{-1} \nabla^2) \mathbf{B} = \nabla \times (\mathbf{U} \times \mathbf{B}), \quad (2.1)$$

$$(\partial_t - \text{Re}^{-1} \nabla^2) \mathbf{U} + \mathbf{U} \cdot \nabla \mathbf{U} = -\nabla p + \mathbf{J} \times \mathbf{B} + \mathbf{F}, \quad (2.2)$$

$$\nabla \cdot \mathbf{B} = \nabla \cdot \mathbf{U} = 0. \quad (2.3)$$

Here \mathbf{U} is the velocity, \mathbf{B} is the magnetic field, p is the pressure, $\mathbf{J} = \nabla \times \mathbf{B}$ is the electric current and Re and R_m are the kinetic and magnetic Reynolds numbers, respectively. The Reynolds numbers are defined by $\text{Re} = ul/\nu$ and $R_m = ul/\eta$ where u and l are typical velocities and lengthscales encountered in the flow and ν and η are the viscous and magnetic diffusivities, respectively. Whilst the latter quantities are fixed for the fluid used in a physical experiment, numerical experiments are free to vary these parameters. We study the effect of varying Re and R_m independently on the solutions calculated here, even though this is not physically realisable in the laboratory.

The system is driven by a forcing function \mathbf{F} chosen to induce (at least initially) a particular velocity in the absence of magnetic effects. We choose this velocity to have desirable kinematic

dynamo properties. The magnetic initial conditions consist of a weak random seed field with amplitude (in units of the velocity) of less than 10^{-5} . The system is then evolved from this initial state of weak magnetisation so that the linear and nonlinear phases of dynamo action can be clearly identified.

Eqs. (2.1)–(2.3) are solved numerically using standard pseudo-spectral techniques (see, e.g., Canuto et al., 1988), with nonlinear terms computed in configuration (coordinate) space and derivatives computed in phase (Fourier) space, where they reduce to simple multiplications. The transformation between configuration and phase spaces is afforded by a (three-dimensional) fast Fourier transform optimised for parallel architecture machines, and the scheme is dealiased by the standard $\frac{2}{3}$ method (Canuto et al., 1988). The time discretisation is a second-order Runge–Kutta scheme, with the diffusive terms included by an integrating factor method. The solenoidality of the magnetic and velocity fields is ensured by an exact spectral projection method. For the typical runs discussed in this paper, adequate resolution was achieved with a maximum of 96^3 Fourier modes.

3. Properties of the flow

Certain properties of the imposed flow are considered to indicate promise for vigorous kinematic dynamo action. In this section, we therefore introduce the family of flows to be considered and investigate their Eulerian and Lagrangian properties.

3.1. Eulerian properties

We consider a modified ABC velocity field defined on a triply periodic Cartesian domain $0 \leq x, y, z \leq 2\pi$ as follows

$$\begin{aligned} U_0 = & (\sin(z + \varepsilon \sin \Omega t) + \cos(y + \varepsilon \sin \Omega t), \\ & \sin(x + \varepsilon \sin \Omega t) + \cos(z + \varepsilon \sin \Omega t), \\ & \sin(y + \varepsilon \sin \Omega t) + \cos(x + \varepsilon \sin \Omega t)). \end{aligned} \quad (3.1)$$

For $\varepsilon=0$, the velocity field (3.1) corresponds to the familiar ABC flow (with $A=B=C=1$). This ABC flow is an example of a steady velocity with chaotic streamlines (Dombre et al., 1986), and has been much studied both in the context of fast dynamo theory (Arnol'd and Korkina, 1983; Galloway and Frisch, 1984; 1986; Lau and Finn, 1993; Galloway and Proctor, 1992; Galloway and O'Brian, 1993) and also in a simple model of a possible route to spatio-temporal turbulence (Zheligovsky and Pouquet, 1993). The flow consists of the superposition of three helical waves and is an example of a flow with the Beltrami property, $\nabla \times \mathbf{u} \propto \mathbf{u}$, and is therefore maximally helical.¹

The steady ABC flows ($\varepsilon=0$) are exact solutions of the Euler equation. However, the flow U_0 is in general time-dependent if ε and Ω are both non-zero. The flow is then essentially the steady ABC flow with its origin moved sinusoidally along the line $x=y=z$ and is thus periodic (in time) with a period $2\pi/\Omega$. The flow is similar to the quasi-two-dimensional time-periodic 'linearly polarized' (LP)

¹ The helicity of a periodic vector field \mathbf{u} is defined by $\mathcal{H} = \langle \mathbf{u} \cdot \nabla \times \mathbf{u} \rangle$, where the angle brackets denote spatial integration over the periodic domain. Maximally helical fields satisfy the equality $\mathcal{H}^2 = \langle |\mathbf{u}|^2 \rangle \langle |\nabla \times \mathbf{u}|^2 \rangle$.

flow considered by Galloway and Proctor (1992). The time dependence is introduced to modify the Lagrangian statistics of the flow and hence possibly its proclivity to dynamo action.

In the presence of viscous dissipation, the flow can be maintained as a solution of the Navier–Stokes equation if a suitable forcing function is chosen. Since \mathbf{U}_0 is both solenoidal and maximally helical, taking $\mathbf{F} = \mathbf{F}_0$, where

$$\mathbf{F}_0 = (\partial_t - \text{Re}^{-1} \nabla^2) \mathbf{U}_0 \quad (3.2)$$

ensures that the flow \mathbf{U}_0 is driven at least in the kinematic regime.

3.2. Lagrangian properties

The dynamo properties of a flow are closely related to its Lagrangian statistics and in particular its chaotic properties (see, for example, Childress and Gilbert, 1995). We therefore examine the Lagrangian statistics of the set of flows defined by Eq. (3.1) for various choices of the parameters ε and Ω , in order to identify potential candidates for efficient kinematic dynamo action. We measure the chaotic properties of the flow in terms of the finite-time Lyapunov exponents, calculated numerically using a procedure based on that described by Soward (1994). These measure the degree of local (exponential) stretching corresponding to chaotic particle paths. The initial conditions for calculating the exponents were distributed uniformly on a (128×128) grid over the plane $z = 0$. Trajectories were then integrated for 30 time units and the largest Lyapunov exponent was calculated. This value was then assigned to the initial position and coded on a grey-scale, where dark tones signify small (or zero) values and light shades represent large and positive values.

3.2.1. Dependence on ε

Fig. 1 shows the (largest) finite-time Lyapunov exponents for the cases $\varepsilon = 0, 0.25, 0.5, 0.75$ and 1 (with Ω fixed at $\Omega = 1$). For $\varepsilon = 0$ (the steady ABC flow) the map is characterised by a thin web of chaos occupying a small fraction of the volume, with much of the flow being integrable. The steady ABC flow (with $A = B = C = 1$) is well known to be weakly chaotic in this manner. If time-dependence is introduced to the flow the regions of chaos grow with increasing ε , with the integrable regions shrinking to small islands. Indeed the average Lyapunov exponent is found to have a monotonic dependence on ε . For $\varepsilon = 1$ the regions of chaotic streamlines occupy almost all of the volume, and thus in the hope of achieving efficient dynamo properties we set $\varepsilon = 1$ for much of the rest of the paper.

3.2.2. Dependence on Ω

The chaotic properties of such modified ABC flows are generally also sensitive to the frequency of the time dependence, Ω (Ponty et al., 1993; Ponty et al., 1995). In Fig. 2 we show the variation of the finite-time Lyapunov exponent map as a function of Ω for $\varepsilon = 1$. For $\Omega = 0$ the flow is steady and so the solution is the same as that for the $\varepsilon = 0$ case shown in the first panel of Fig. 1. As soon as the flow becomes time-dependent, the regions of chaos expand until the extent of chaos (as measured by the Lyapunov exponent at least) appears to reach a maximum at $\Omega = 1.5$. The islands of integrability regrow if Ω is increased past this value, and for $\Omega = 4$ the chaotic regions have shrunk significantly, leaving substantial regions where the flow is integrable once again. This behaviour can be quantified by calculating the average and maximum Lyapunov exponents as functions of Ω as

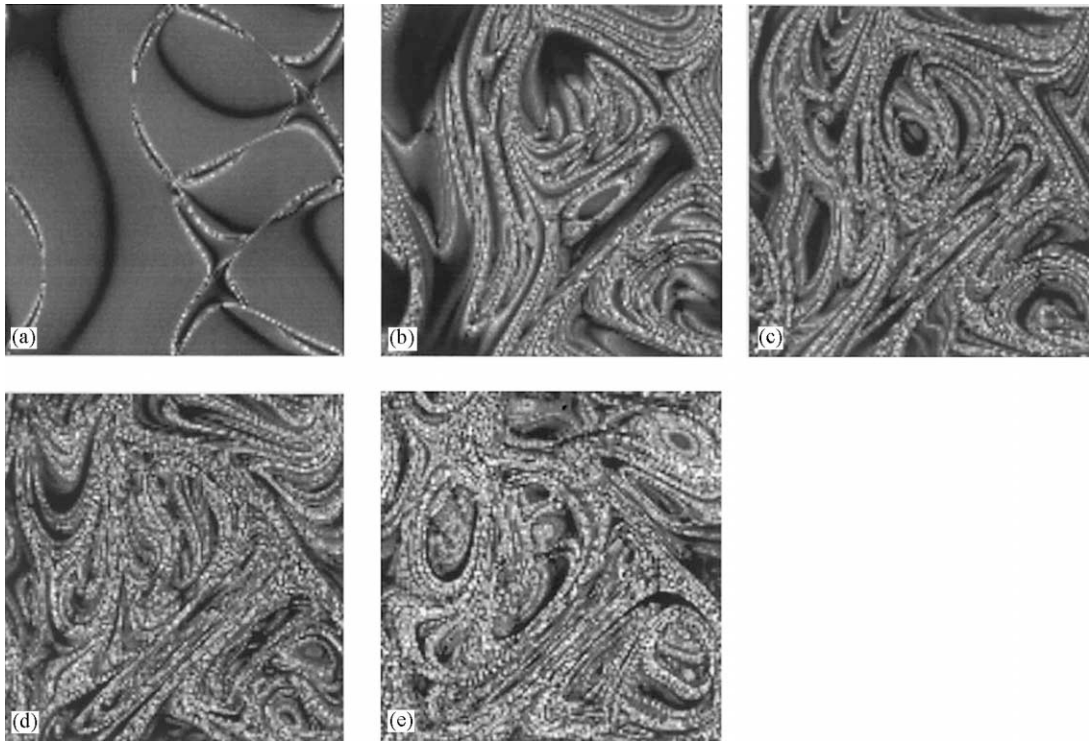


Fig. 1. Grey-scale maps of the finite-time Lyapunov exponents for U_0 with $\varepsilon =$ (a) 0, (b) 0.25, (c) 0.5, (d) 0.75, (e) 1 and $\Omega = 1$. Values range from zero (black) to between 0.25 and 0.30 (white).

shown in Fig. 3. It is clear from both these measures that the levels of chaos grow to a maximum as Ω increased and decrease as Ω takes on larger values. Whether this maximum occurs at $\Omega = 1.0$ or 1.5 depends on the specific measure. We might expect to see a similar dependence in the kinematic growth rates for dynamo action as Ω is varied.

3.3. Hydrodynamic stability

The initial hydrodynamic flow is chosen for the properties outlined above and its stability properties. It is unfortunate that such flows tend to be hydrodynamically unstable at the Reynolds numbers considered. It is helpful though if the hydrodynamic instability acts in a such a manner that the flow remains close to the original flow whilst the dynamo action of interest takes place. This is indeed the case for the flows studied in this paper, as illustrated in Fig. 4. The purely hydrodynamic evolution of the flows ($\varepsilon = 1, \Omega = 2.5$) for $Re = 40, 60, 90$ has been calculated including a small perturbation to the velocity, and the time history of the kinetic energy is illustrated. It can be seen in the example cases shown that these time series eventually deviate from the value of three (corresponding to U_0), indicating instability. However, the onset of this instability does not take place until 100 time units or more have passed. In what follows, this is more than ample time in general for dynamo action to amplify the magnetic field and for the nonlinear regime to begin. The growth rate of the

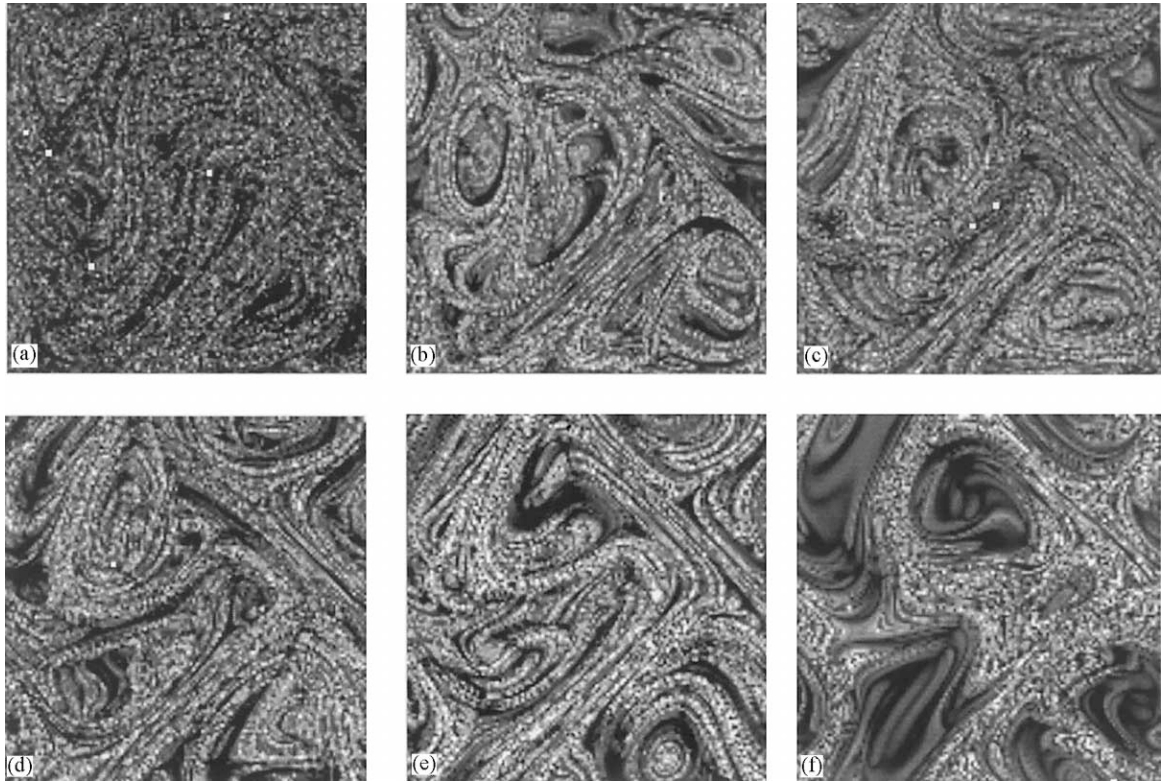


Fig. 2. Grey-scale maps of the finite-time Lyapunov exponents for U_0 with $\Omega =$ (a) 0.5, (b) 1.0, (c) 1.5, (d) 2.0, (e) 2.5, (f) 4.0 and $\varepsilon = 1$. Average and maximum values are shown in Fig. 3.

hydrodynamic instability increases with increasing Re , and, at least for sufficiently high Re ($Re > 50$ in Fig 4), the final hydrodynamic state appears to be chaotic. The exact nature of the bifurcation structure for this hydrodynamic system would require deeper investigation (of the type found in Podvigina and Pouquet (1994) and Podvigina (1999)) and is not the primary thrust of this paper. Our hydrodynamic investigations have determined that instability will occur in this manner for all $Re > 17$, at least for $\varepsilon = 1$, $\Omega = 2.5$. Thus, for almost all the kinetic Reynolds numbers contained in this paper, U_0 is unstable, yet in this relatively slow manner.

4. Kinematic regime

Since much work has considered the kinematic dynamo properties of certain velocity fields such as U_0 , we wish to understand the relationship, if any, between the nonlinear MHD regime and the linear kinematic regime. Though our model is inherently always nonlinear, the fact that the calculations start from a state of weak magnetisation and the hydrodynamic instability of the chosen flow is slow means that there exists a regime early on in the simulations where the flow remains close to U_0 and the Lorentz force is negligible. Here, the dynamo action is effectively kinematic, and the magnetic energy grows exponentially with a well-defined growth rate. This regime can be identified in the

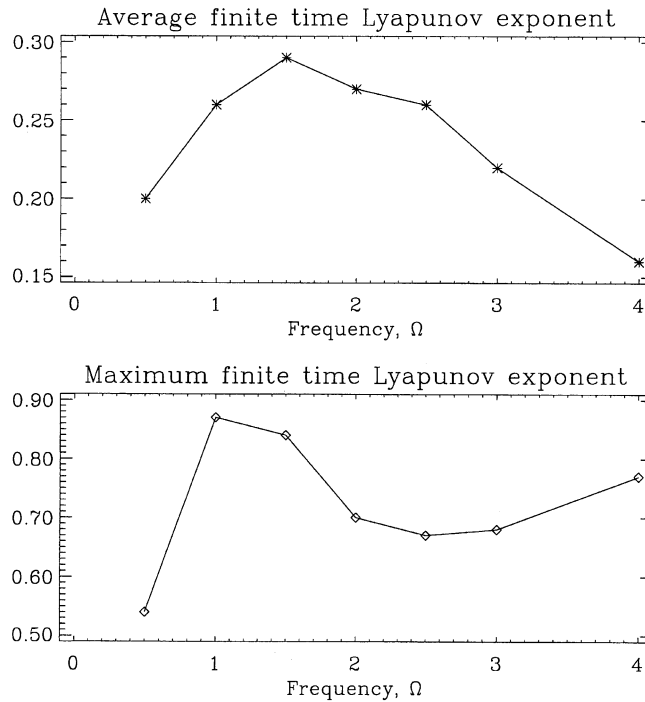


Fig. 3. The variation with Ω of the average and maximum finite-time Lyapunov exponents for \mathbf{U}_0 with $\varepsilon = 1$.

simulation by choosing that time interval where the kinetic energy remains within a few percent of the initial value of the kinetic energy ($=\frac{3}{2}$). In this section, we discuss the dynamo properties of the flows in this effectively kinematic regime, in a similar manner to other kinematic investigations of steady and unsteady ABC flows (Ponty et al., 1993; Ponty et al., 1995; Galanti et al., 1993). We stress again, however, that here this regime is identified from a fully nonlinear simulation in a state of weak magnetisation, and not calculated kinematically with a prescribed velocity.

4.1. Dependence of growth rate on ε

We begin by investigating the kinematic properties of the dynamo as a function of the amplitude of oscillation ε . For this section, the other fluid parameters are held fixed at $R_m = Re = 100$ and $\Omega = 1$. The resulting time series showing the linear growth of the magnetic energy from the small seed field for various values of ε are shown in Fig. 5. It is clear from this figure that two different types of behaviour are possible. If $\varepsilon = 1.0$ or 0.75 the magnetic energy grows exponentially with a well-defined growth rate throughout the whole linear phase. However, for $\varepsilon \leq 0.5$ the exponential growth of the magnetic field stops after a while and the field then grows in a more complicated manner. This can be understood in terms of the hydrodynamic stability of \mathbf{U}_0 discussed previously, where it was shown that the flow remained close to the original ABC flow for about 100 time units or more (although the growth rates may be somewhat different for different ε). For the higher ε , the linear phase completes in this time (the vertical dotted line in the upper panel) with the flow remaining close to \mathbf{U}_0 , but for the lower ε where the magnetic growth rate is slower, it does not.

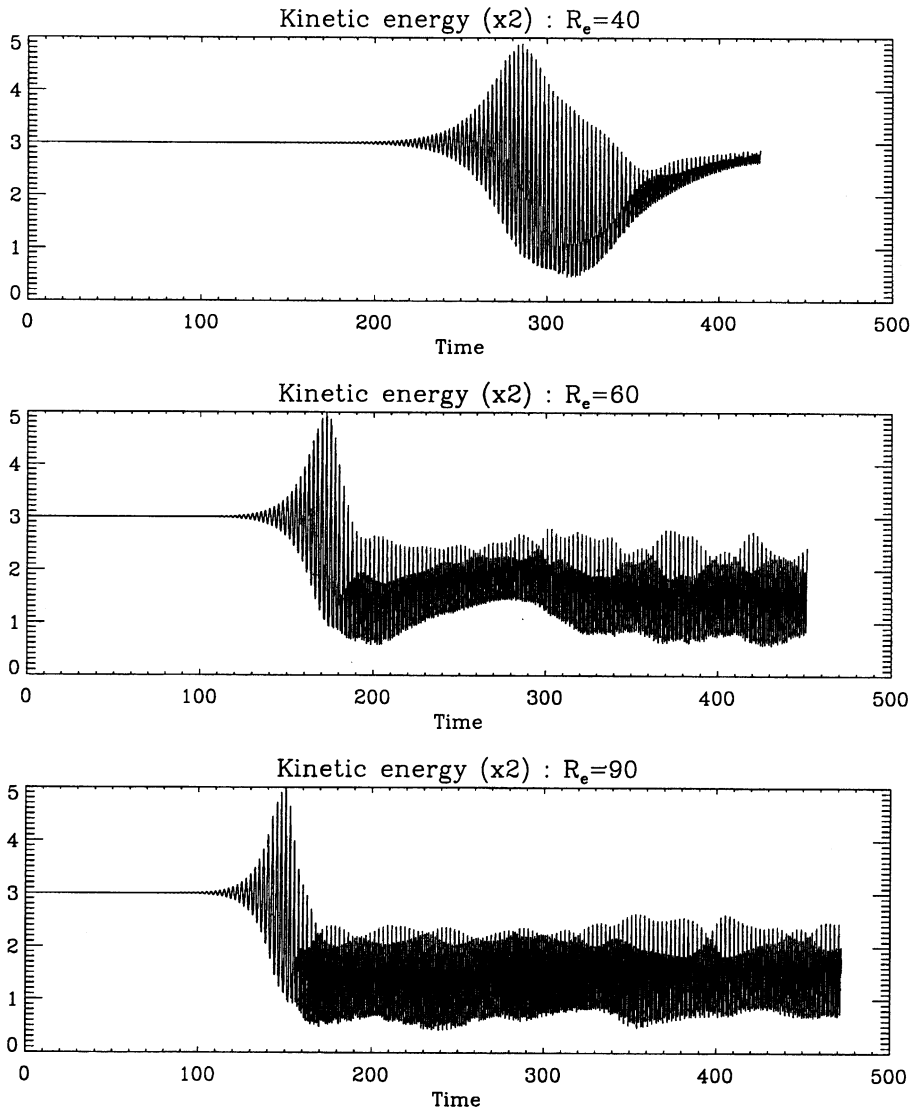


Fig. 4. Time traces of the kinetic energy (times 2) for purely hydrodynamic cases with $Re = 40, 60, 90$ and $\varepsilon = 1, \Omega = 2.5$, illustrating the onset of instability after a relatively long interval of at least 100 time units. The instability saturates in an apparently chaotic hydrodynamic state for $Re = 60$ and 90 .

After approximately 100 time units, in the former case, the solution has reached a full MHD state, whereas in the latter case, the velocity field has become unstable to one which has very different dynamo properties from the initial ABC flow (vertical dotted line in lower panel), and the field is then amplified more slowly and in an irregular manner. In this regime (between the vertical dotted and dashed lines in the lower panel for $\varepsilon = 0.25, 0.5$), the magnetic field is small and so it is unlikely that the Lorentz force is playing a significant role in modifying the flow; it is more likely that the hydrodynamic instability has caused the change in growth rate. For these ε , the Lorentz force

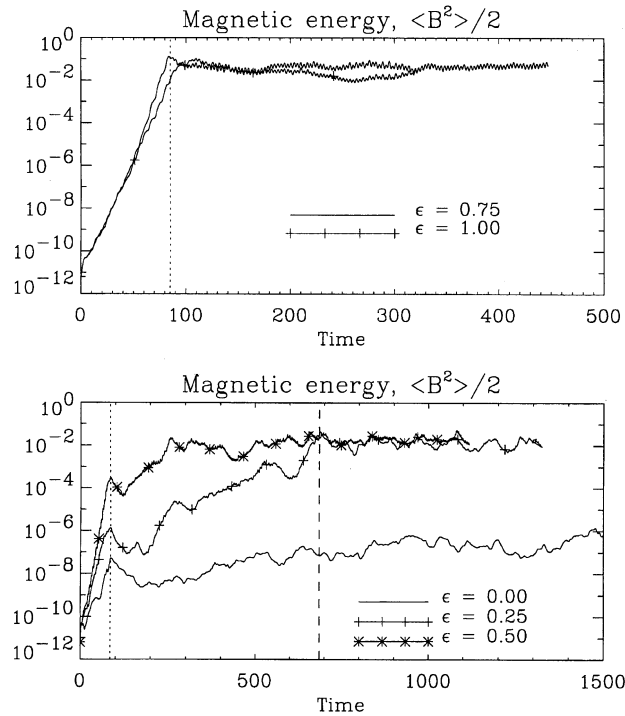


Fig. 5. The growth of the magnetic energy versus time for various ε with $\Omega=1$ and $R_m=Re=100$: upper panel $\varepsilon=0.75, 1.0$, lower panel $\varepsilon=0.0, 0.25, 0.5$. In the upper panel, the vertical dotted line separates the exponential kinematic growth phase from the nonlinear regime. In the lower panel, the linear phase is more complicated, with two sections: an exponential growth to the left of the dotted line again, and a more complex amplification up until nonlinear saturation at the vertical dashed line (at least for $\varepsilon=0.25, 0.5$).

eventually becomes significant at the dashed vertical line and nonlinear saturation occurs. For $\varepsilon=0$, the growth rate of the modified flow (occurring after the dotted line) is very small, and nonlinear equilibration does not occur in the time shown in the figure. The rest of this paper concentrates on the straightforward case with $\varepsilon=1$, where the kinematic growth rate is better defined.

4.2. Dependence of growth rate on Ω

The linear phase of dynamo action is shown in Fig. 6 for various choices of the frequency of the oscillation of the flow. The amplitude of the oscillation of the flow is now held fixed at $\varepsilon=1$ and $R_m=Re=100$, with the frequency of oscillation ranging from $\Omega=0.5$ to 4.0. For all the values of Ω considered, the magnetic energy grows exponentially with a well-defined growth rate σ . For these parameters, the periodic ABC flow is certainly effective in generating field throughout the linear phase of dynamo action.

The growth rate for $\langle B^2 \rangle$ is plotted against Ω also in Fig. 6. The growth rate σ does not have a simple (monotonic) dependence on frequency; there is an optimum frequency of oscillation for kinematic dynamo action. This maximum occurs near $\Omega=2.5$, with the growth rate decreasing in both the low- and high-frequency limits. This behaviour is reminiscent of that of the Lyapunov

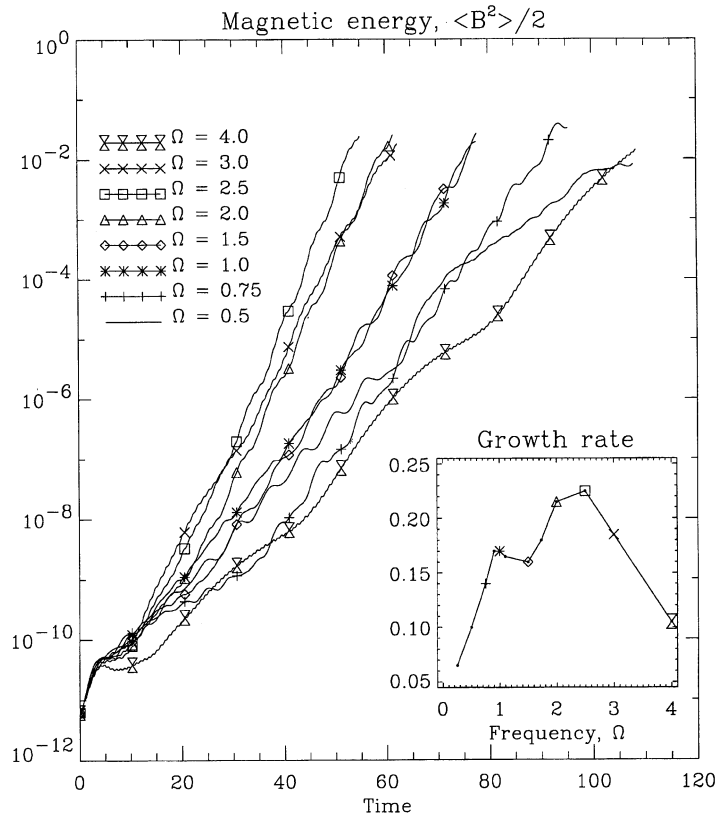


Fig. 6. Growth of the magnetic energy versus time in the kinematic phase of the dynamo for various Ω with $\varepsilon = 1$ and $R_m = Re = 100$. Inset: The measured linear growth rate of the magnetic energy versus Ω , including the example cases shown in the main figure.

exponents outlined in Section 3.2.2, where the chaotic properties of the flow (as measured by both the maximum and average Lyapunov exponents) were found to depend critically on the frequency of the flow. However, comparison of the dependence of σ and the Lyapunov exponents on Ω shows that the maximums occur at different frequencies. This confirms that although the Lyapunov exponent yields a measure of the chaotic properties of the flow, it is not a true indicator of the ability of the flow to generate magnetic fields. The Lyapunov exponent only measures the local stretching properties of the flow and does not give any indication of the self-cancellation of the generated magnetic fields. Similar kinematic results for other flows have been found by Cattaneo et al. (1995), and by Ponty et al. (1993) (see also Ponty et al., 1995), who also suggest that the Melnikov method should be used to gain a better measure of a flow’s efficiency at generating magnetic field.

4.3. Dependence of growth rate on R_m

We consider here the dependence of the growth rate σ with R_m . Much attention has been devoted to the question of kinematic field amplification in the limit $R_m \rightarrow \infty$ – the fast dynamo limit. It is now known that flows that are not too symmetric and with chaotic trajectories occupying a substantial

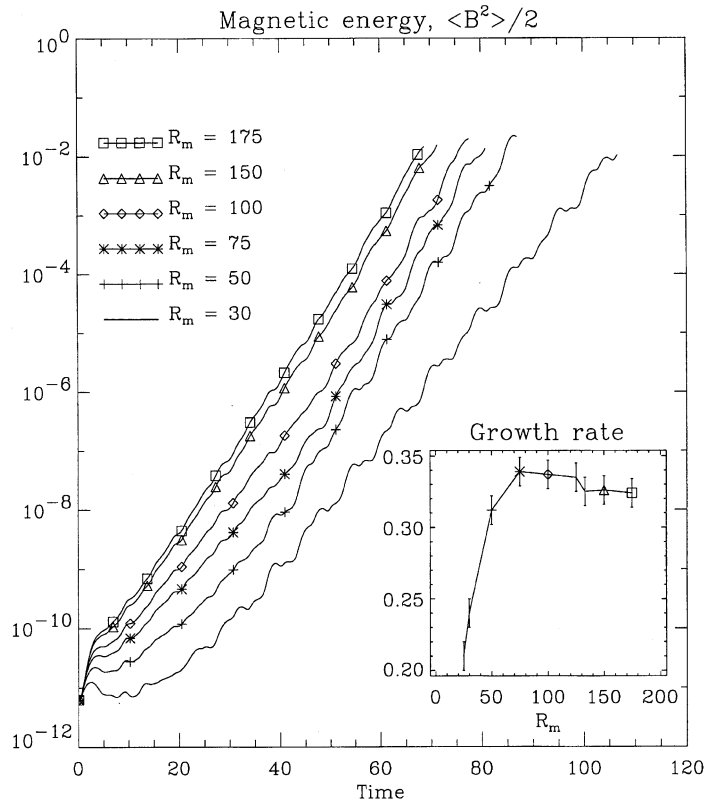


Fig. 7. Growth of the magnetic energy versus time in the kinematic phase of the dynamo for various R_m with $\varepsilon = \Omega = 1$ and $Re = 50$. Inset: The measured linear growth rate of the magnetic energy versus R_m , including the example cases shown in the main figure. The error bars give some indication of the variation of the growth rate depending on exactly how it is measured.

fraction of the volume are likely candidates for fast dynamo action (Childress and Gilbert, 1995). The family of velocity fields under consideration here fall within this class of flows and are therefore likely to possess the fast dynamo property. However, by necessity, most nonlinear studies, including this one, are restricted to moderate values of R_m and cannot directly address the fast dynamo issue. The important property for the present study is that the dynamo remains kinematically efficient (i.e. rapidly growing) for the range of magnetic Reynolds numbers under consideration. The reason for choosing a velocity that is likely to be a fast dynamo is that it lends some support to our expectations that the results obtained at moderate magnetic Reynolds numbers may also apply asymptotically to the small diffusivity limit.

Fig. 7 shows the kinematic growth of magnetic energy when the forcing is fixed ($\varepsilon = \Omega = 1$) and R_m is varied. This figure shows that for all the parameter values considered, the magnetic energy grows exponentially with a well-defined growth rate, and then this growth rate σ is plotted as a function of R_m . For small values of R_m , the growth rate is an increasing function of R_m , but for R_m sufficiently large ($R_m > 50$) the growth rate becomes relatively independent of R_m and the kinematic behaviour appears to have reached an asymptotic regime. We note that this behaviour is similar to that of the ABC-type flows studied by Galloway and Proctor (1992).

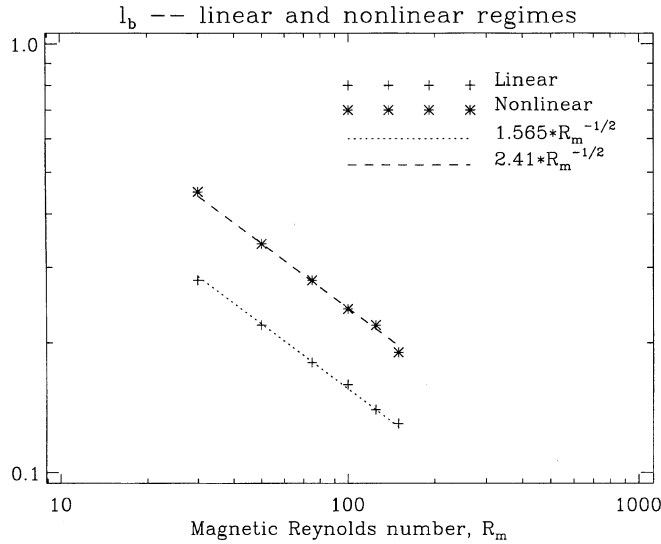


Fig. 8. The magnetic lengthscale, l_b , plotted as a function of R_m for $\varepsilon = \Omega = 1$ and $Re = 50$. Both in the linear and nonlinear regimes, l_b appears to scale as $R_m^{-1/2}$.

4.4. The lengthscale of the magnetic field

It is instructive to investigate the scalings of the structure of the generated field for fixed ε and Ω (since these are expected to have a weak influence on the form of the magnetic field) and to concentrate on the changes in the nature of the driven field as R_m is varied. An average measure of the lengthscale of the magnetic field is given by

$$l_b = \left(\frac{\langle B^2 \rangle}{\langle j^2 \rangle} \right)^{1/2}, \tag{4.1}$$

where $\langle \cdot \rangle$ represents an average of the quantity over the computational domain. This is a measure for the magnetic field equivalent to the Taylor microscale for the velocity field. Fig. 8 shows the variation of l_b extracted from the simulations in the kinematic regime (and also in the nonlinear regime for later use) with the imposed magnetic Reynolds number R_m . The plot shows that there is a power-law dependence and the line of best fit demonstrates that $l_b \propto R_m^{-1/2}$ for all values of R_m investigated. This scaling is not surprising in this kinematic regime however, since the forcing is chosen so that the velocity is imposed with $\mathcal{O}(1)$ magnitude and lengthscale, and therefore the scaling of the magnetic field follows from a balance of advection and diffusion in the induction equation.

5. Nonlinear Regime – dynamo equilibration

Having considered the kinematic regime, where magnetic perturbations had little influence on the forced velocity field, we now consider the *nonlinear regime* where the back-reaction of the magnetic field on the flow (via the nonlinear Lorentz force) becomes significant.

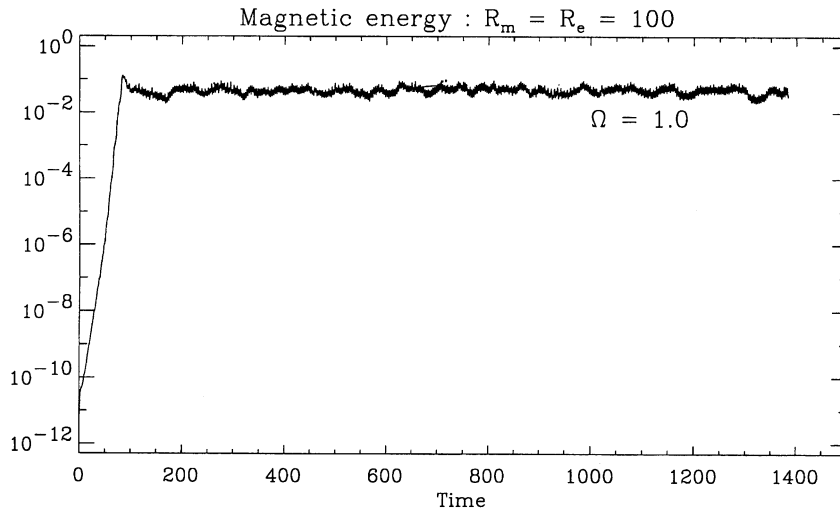


Fig. 9. A plot of typical dynamo saturation. Here, the magnetic energy is plotted against time for the case with $\Omega = \varepsilon = 1$ and $R_m = R_e = 100$, and the full time series including the linear and nonlinear regimes is shown.

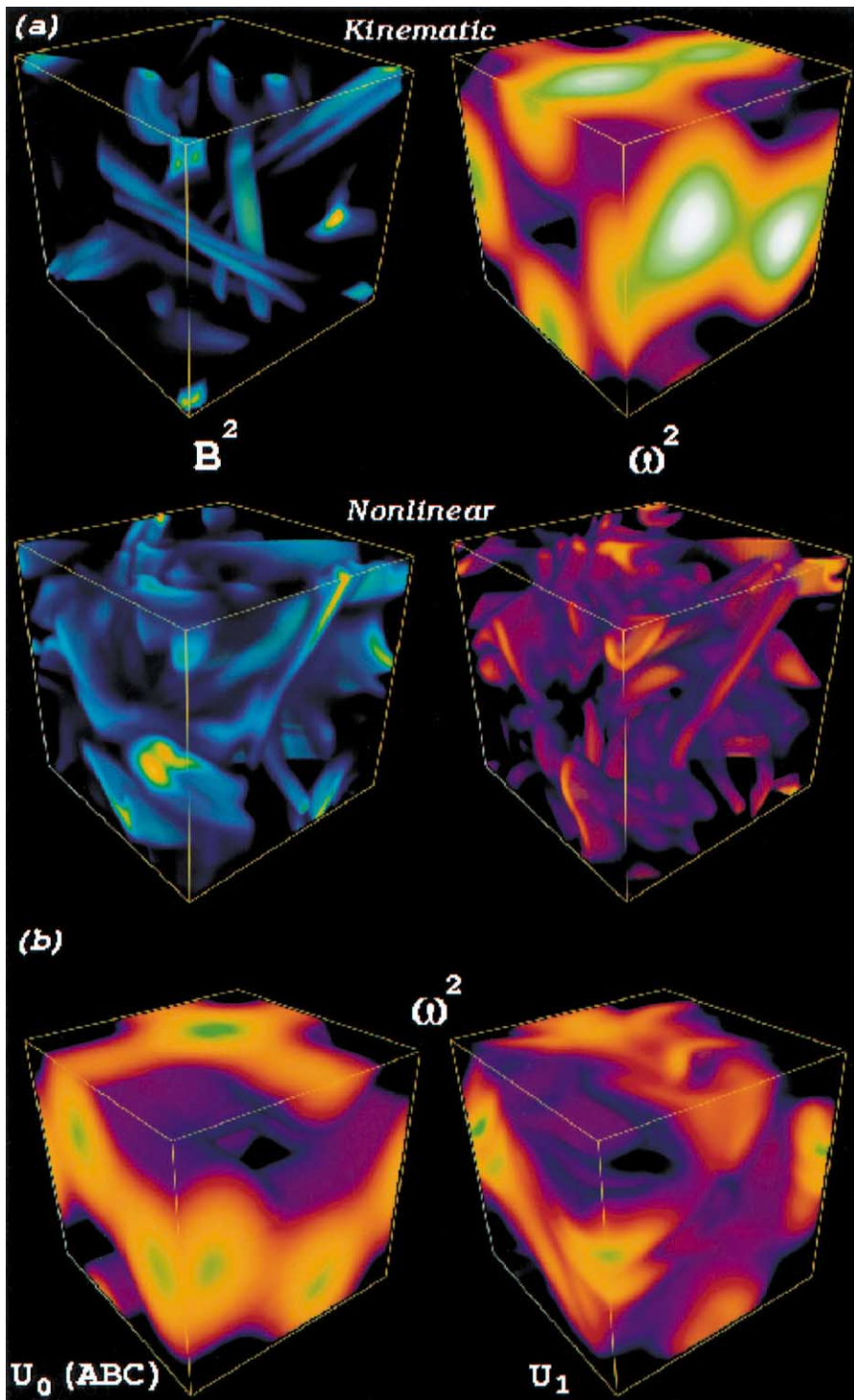
First, we consider the case $\varepsilon = \Omega = 1$ where the dynamo behaves “normally” in the nonlinear regime, i.e. the magnetic perturbations adjust the velocity field, via a balance between the Lorentz force and the applied driving, such that the magnetic field growth saturates at a finite amplitude. This simple saturation is not the only possible outcome in the nonlinear regime, and we describe more complex outcomes in the next section.

5.1. Structure of the dynamic fields

Fig. 9 temporal evolution of the magnetic energy for a calculation with $R_m = R_e = 100$. Here the initial exponential growth of magnetic energy in the kinematic regime is clearly exhibited by a straight line in the logarithmic plot. When the magnetic energy becomes large enough (in this case when $\langle B^2 \rangle \approx 10^{-1}$), the magnetic energy ceases to grow, and (after a brief period of readjustment) the solution settles down to a statistically steady state where the magnetic field neither grows nor decays. This scenario represents the traditional view of the operation of a dynamo.

Fig. 10(a) exhibits the adjustment of the magnetic and velocity fields associated with this saturation process. This figure shows volume renderings of magnetic energy and enstrophy density (B^2

Fig. 10 (a) Volume renderings of the magnetic energy and enstrophy densities for the typical dynamo saturation case with $\Omega = \varepsilon = 1$ and $R_m = R_e = 100$. For the rendering, each value is assigned a colour and an opacity, with high values being bright and opaque (green–yellow–white) and low values being dark and translucent (black–blue–purple). The upper half of the figure shows the fields extracted from the linear regime, where the enstrophy still resembles that of the initial ABC flow U_0 and the magnetic energy is close to that of the kinematic eigenfunction. The lower half shows a typical time in the nonlinear regime where the fields are now distinctly different from the kinematic versions. (b) Volume renderings of the enstrophy density for the flows U_0 and U_1 at typical times in their time-dependent evolutions. It is clear that the lengthscale for U_1 is shorter than that for U_0 .



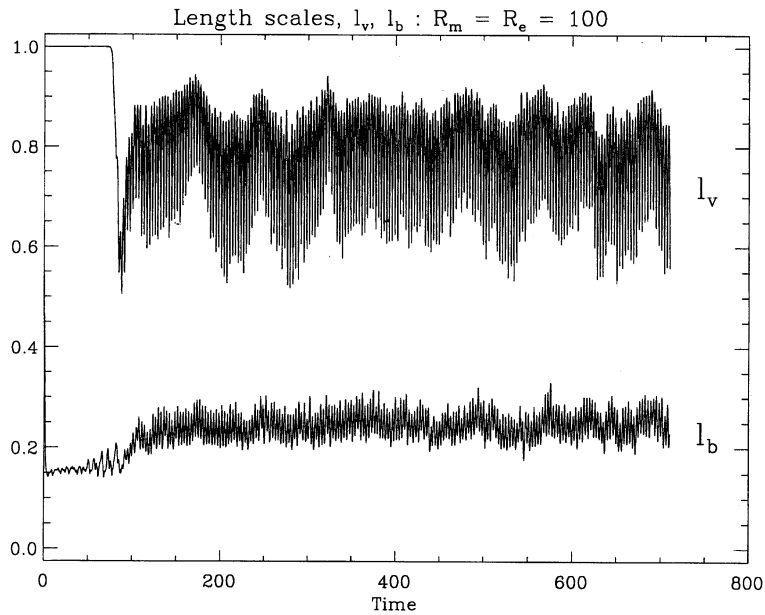


Fig. 11. A plot of the velocity and magnetic lengthscale measures, l_v and l_b , against time for the case of typical dynamo saturation with $\Omega = \varepsilon = 1$ and $R_m = R_e = 100$.

and ω^2 , where $\omega = \nabla \times \mathbf{U}$, the vorticity). The upper panels of Fig. 10(a) show a representative time during the kinematic phase, whereas the lower panels exhibit the nonlinear phase. The kinematic eigensolution for the magnetic field takes the form of tubes (or cigars) which grow in strength exponentially. In the nonlinear regime, the structure of the field changes, replacing the simple tube-like structures of the linear regime by a mixture of magnetic tubes and sheets, and the field appears to have a higher filling factor than in the kinematic regime. This change in lengthscale engendered by the change from tubes to tubes and sheets can also be seen in the time series for l_b (defined in Eq. (4.1)) in Fig. 11. As the solution enters the nonlinear regime at $t \sim 75$, the lengthscale of the magnetic field increases (discussed further in Section 5.2.1).

The magnetic field has acted to modify the velocity field in such a way that the resulting flow acts as a statistically marginal dynamo. That the velocity has been altered is clear on viewing the snapshots of enstrophy in the linear and nonlinear regimes which are given in Fig. 10(a). In the kinematic regime, the velocity has not been modified significantly from the forced ABC flow and the enstrophy shows that the velocity consists of structures that vary on the lengthscale of the computational domain. However, in the nonlinear regime the velocity is much less regular and the spatial scale of the flow has decreased. This velocity field has contributions resulting from driving by both the imposed and Lorentz forces. Unfortunately, because the flow is no longer a Beltrami flow (i.e. $\mathbf{U} \times \omega \neq 0$) and is now nonlinear, it is impossible to separate out the flow into these two constituent components and to examine the properties of these independently. However, a measure of the lengthscale of the flow can be gained by examining the time series (Fig. 11) of the Taylor

microscale defined to be

$$l_v = \left(\frac{\langle v^2 \rangle}{\langle \omega^2 \rangle} \right)^{1/2}. \quad (5.1)$$

This figure does indeed show that the lengthscale of the velocity decreases from the kinematic value, unity, when the solution enters the nonlinear regime.

5.2. Scaling with R_m and Re

We now repeat the calculation performed in the previous section for a number of choices of R_m and Re , in order to elucidate some scaling properties for nonlinear dynamo action. In each case the dynamo solutions show behaviour similar to that discussed above for $R_m = Re = 100$.

5.2.1. Dynamic magnetic lengthscale

In the kinematic regime, the lengthscale of the magnetic eigenfunction scales as $R_m^{-1/2}$, demonstrating a balance between advection and diffusion of the magnetic field. Fig. 8 shows the dependence of the lengthscale l_b on R_m , calculated by averaging over a long period of integration in the nonlinear regime. The figure demonstrates that in the nonlinear regime the magnetic lengthscale continues to scale as $R_m^{-1/2}$ (for Re fixed). Thus, for all values of R_m considered, despite a jump in magnetic lengthscale that occurs as the field enters the nonlinear regime, the scaling of the field with R_m is maintained, and only the coefficient of proportionality changes. In contrast, the magnetic lengthscale does not appear to depend at all on the value of Re (at least for the values of Re considered here). This indicates that, even in this highly nonlinear regime, where the structure of the magnetic field is very different from that in the linear regime, the magnetic lengthscale is still determined by a balance of advection and diffusion in the induction equation. After modification such that a statistically steady marginal dynamo is achieved on entering the nonlinear regime, the velocity field must effectively return to being an input to the induction equation so that the balance between advection and diffusion is restored.

It must be stressed that the scalings for the nonlinear magnetic lengthscale are found for reasonably small values of R_m and Re , and that it would be dangerous to extrapolate these to larger values. If the Reynolds number of the flow is increased significantly, one might expect nonlinear fluid effects to become more important and the lengthscale to show a greater dependence on Re . However, the scaling exhibited does continue to the highest values of R_m considered. This gives some hope that behaviour of the nonlinear solutions may not be too different in the small diffusivity limit.

5.2.2. Magnetic energy

A central question in dynamo theory is how surprisingly strong (small-scale and mean) magnetic fields may be generated by the transfer of energy from the velocity into the magnetic field. It is of consequence therefore to examine how large the magnetic field in the simulations can become before the effects of the Lorentz force lead to equilibration and a resulting saturated value of the energy.

Fig. 12 shows the variation of the average magnetic energy $\langle B^2 \rangle$ with R_m (averaged over a long period in the nonlinear regime) for fixed Reynolds number Re . The dependence of the magnetic energy on R_m in the nonlinear regime closely reflects that of the kinematic growth rate. For small

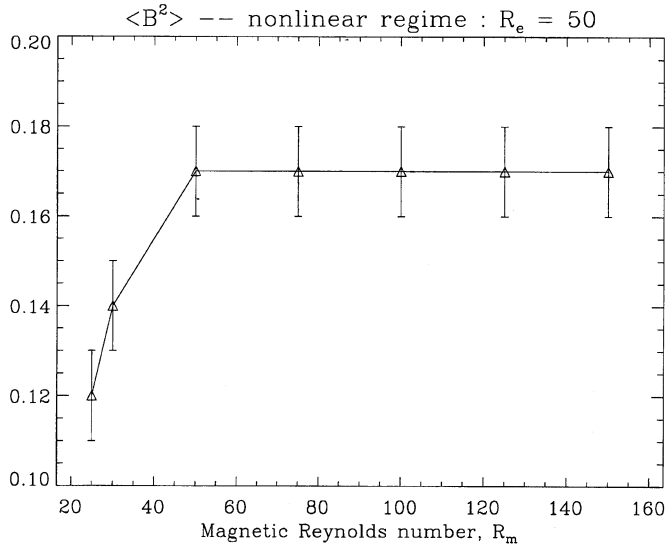


Fig. 12. A plot of the average saturated value of the magnetic energy against R_m for cases with $\Omega = \varepsilon = 1$ and $Re = 50$. Error bars show the maximum variation incurred by calculating the average from different portions of the nonlinear regime.

values of R_m the average magnetic energy increases with R_m , and here, where magnetic diffusion is important, the numerical results are consistent with a scaling of $\langle B^2 \rangle \propto R_m^{1/2}$. However, as R_m is increased the dependence plateaus, and the average magnetic energy becomes independent of R_m . It therefore seems that in this case the kinematic growth rate can act as a useful indicator of the saturation of the dynamo.

In the nonlinear regime, the Lorentz force becomes significant relative to the imposed forcing and viscous diffusion terms. The balance between these terms is controlled by the fluid Reynolds number, Re , and so we show the dependence of the average saturated magnetic energy on Re in Fig. 13. The magnetic energy has a power-law dependence on the viscous diffusion consistent with the scaling $\langle B^2 \rangle \propto Re^{-1}$.

The above dependences in the lower Re , R_m regimes may be explained by considering the balance between the magnetic Lorentz force and the imposed forcing and viscous diffusion in the Navier–Stokes equation. The prescribed forcing is chosen so that in the absence of magnetic field the same ABC flow of unit amplitude (i.e. $A = B = C = 1$) is always driven, and therefore the forcing is dependent on Re . In the low Re limit, or where the Beltrami property still holds somewhat, $U \cdot \nabla U$ can be ignored and so in a long time average

$$F = F(Re) \sim \frac{1}{Re} \nabla^2 U_F \sim \frac{1}{Re} \frac{U_F}{l_{U_F}^2} \sim \frac{1}{Re} \tag{5.2}$$

since the characteristic amplitude and lengthscale of the imposed velocity U_F , l_{U_F} are both $\mathcal{O}(1)$.

When the magnetic field is present the velocity comprises two parts – a flow imposed by the forcing described above, and a flow driven by the magnetic Lorentz force; i.e. $U = U_F + U_M$. In the low Re limit, nonlinear interactions between these two flows are ignored and the Navier–Stokes equation can be decomposed into two separate equations for U_F and U_M . The equation for U_F is

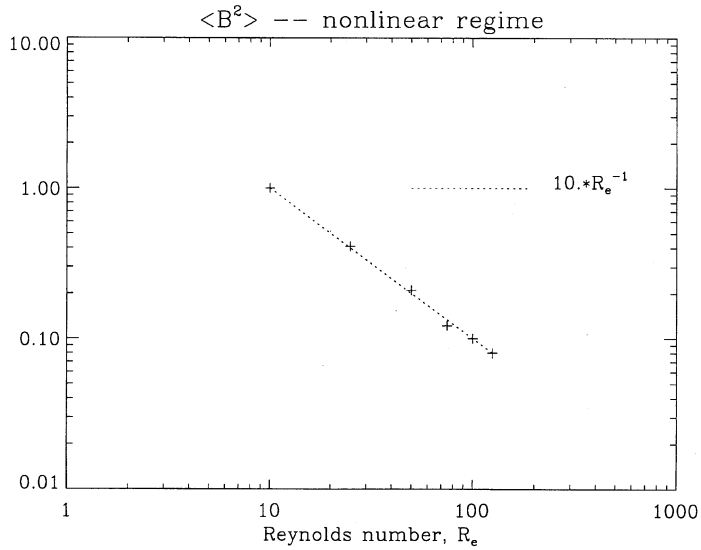


Fig. 13. The variation of the average saturated value of the magnetic energy with Re for cases with $\Omega = \varepsilon = 1$ and $R_m = 100$. The values are consistent with a scaling proportional to Re^{-1} .

satisfied by the balance proposed in Eq. (5.2). The magnetically driven flow is given by balancing the Lorentz force with viscous diffusion, i.e.

$$(\nabla \times \mathbf{B}) \times \mathbf{B} \sim \frac{1}{Re} \nabla^2 \mathbf{U}_M \tag{5.3}$$

$$\Rightarrow \frac{B^2}{l_b} \sim \frac{1}{Re} \frac{U_M}{l_{U_M}^2} \tag{5.4}$$

The size and lengthscale of the magnetically driven velocity U_M are difficult to determine from the calculations since the only sensible lengthscale that may be calculated is the Taylor microscale l_v , and, as noted earlier, this cannot be easily related to either l_{U_M} or l_{U_F} . A rough estimate may be gained however by assuming that the magnetically driven velocity reaches an amplitude where its contribution to the induction equation is comparable to that of U_F , i.e. $U_M \sim U_F \sim \mathcal{O}(1)$. Moreover, U_M is driven by the quadratic Lorentz force generated by a field with lengthscale l_b . In this case, one would expect

$$l_{U_M} \sim \frac{1}{2} l_b \sim R_m^{-1/2} \tag{5.5}$$

and substituting into Eq. (5.4) one finds that

$$B^2 \sim R_m^{1/2} Re^{-1} \tag{5.6}$$

The scaling we derive is similar to that derived by Galloway et al. (1978) for Boussinesq magnetoconvection. Eq. (5.6) appears empirically to be valid only for small values of R_m . As mentioned earlier, as R_m is increased the equilibration energy of the magnetic field becomes insensitive to changes in diffusion. This must imply that one of the assumptions used in deriving the scaling (i.e. negligible inertia forces, $U_M \sim U_F$) breaks down as R_m is increased. Moreover, one would expect the scaling to break down as Re is increased (although this has not been observed) as the primary

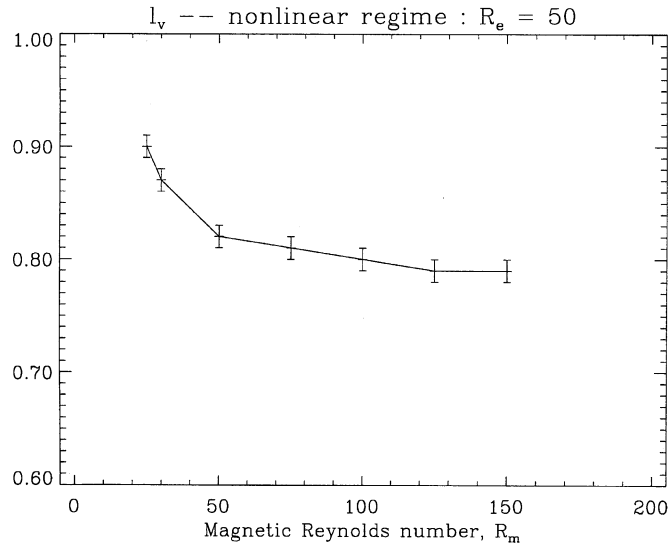


Fig. 14. The variation of the velocity lengthscale, l_v , in the nonlinear regime with R_m for cases with $\Omega = \varepsilon = 1$ and $Re = 50$. The error bars show the maximum error in calculating l_v over different portions of the nonlinear regime.

balance in the momentum equation would then have to include the nonlinear advection term. It appears as though two different mechanisms for saturation occur. For small R_m , saturation depends on diffusion, and the magnetic energy scales as demonstrated above. As R_m is increased, the level of saturation becomes independent of diffusion and a more subtle process (e.g. suppression of chaos by the magnetic field, as in Cattaneo et al., 1996) may be occurring.

Within the confines of the approximation, it would seem as though one may generate a field of any given energy simply by decreasing Re to an appropriate level. This is counterintuitive since it is not immediately apparent where the extra energy is coming from. The explanation is that the flow is generated by a prescribed forcing where, for all values of Re , the *same* velocity is generated. In the limit of large diffusion the forcing needs to be larger to overcome the dissipation and to generate the required flow. Thus, more energy is being injected into the system and is available to be converted into magnetic energy.

5.2.3. Velocity lengthscale

It was noted in the previous section that the fluid velocity in the fully nonlinear MHD state is driven both by the imposed forcing and the magnetic Lorentz force. The forcing is designed to generate a fluid velocity with a lengthscale of order unity (as shown in the linear portion of Fig. 11). The magnetically driven perturbations change the lengthscale of the flow but not in a manner that is easily accessible to scaling laws, since U_M and U_F are inextricably related. Fig. 14 shows the dependence of l_v on R_m . For small magnetic Reynolds number, l_v varies with R_m but, as for the magnetic energy, this sensitivity to R_m decreases as R_m is increased. The explanation for this behaviour is due to the indirect dependence of l_v on R_m via both U_M and l_b . We described earlier how the magnetic energy of the equilibrated solutions increased with increasing R_m until a plateau was reached for R_m sufficiently large. This implies that as R_m is increased, the relative importance of the

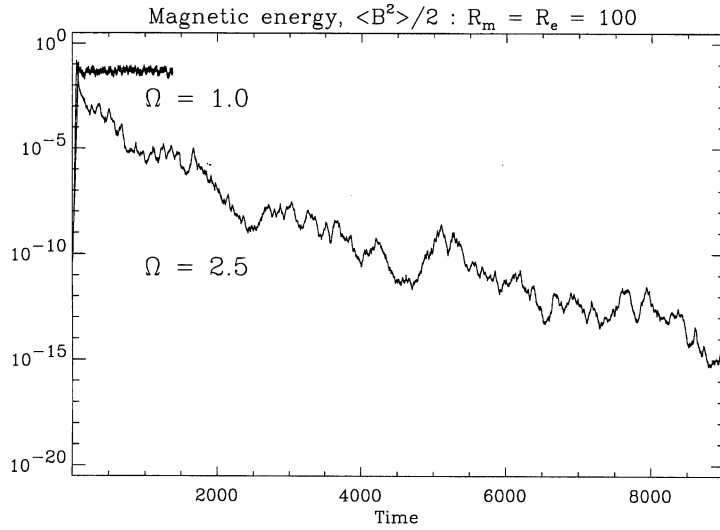


Fig. 15. A plot of the magnetic energy versus time for the two contrasting cases, $\Omega = 1.0$ and 2.5 , where $\varepsilon = 1$ and $R_m = R_e = 100$, including both the linear and nonlinear regimes.

magnetically driven velocity (U_M) to the driven ABC flow (U_F) increases, decreasing the average measure l_v away from unity. This effect saturates because the magnetic energy reaches a plateau and the magnitude of U_M becomes independent of R_m . However, the lengthscale of U_M continues to change in a similar manner to l_b (i.e. scaling as $R_m^{-1/2}$). Thus the dependence of l_v on R_m weakens as R_m is increased although small changes in l_v can still be detected.

6. Nonlinear Regime – A nondynamo

The equilibration to a statistically marginal dynamo, as described in the previous section, is the scenario traditionally envisaged for the nonlinear dynamo. In this section, we examine a case that exhibits dramatically different nonlinear behaviour. We follow the evolution of the case with the best kinematic dynamo activity (maximal growth rate in the kinematic regime), at parameters $\varepsilon = 1$, $\Omega = 2.5$, $Re = R_m = 100$, and contrast this with the case exhibited in the previous section, where $\Omega = 1$.

6.1. Nonlinear behaviour for $\Omega = 2.5$

Fig. 15 compares the behaviour in the linear and nonlinear regime for cases with $\Omega = 1$ and $\Omega = 2.5$. For the latter case, the magnetic energy increases kinematically until $t \sim 70$ where $\langle B^2 \rangle \sim 10^{-1}$. The growth rate is faster than the $\Omega = 1$ case, as found before, and so the solution reaches the saturations magnetic energy amplitude more quickly. However, after this point, remarkably the field immediately begins to decay instead of equilibrating as in the $\Omega = 1$ case, and indeed eventually decays away to values smaller than the original seed field. For this value of the forcing parameters the induced flow is therefore *not* ultimately a dynamo since field is not maintained at a finite values for all time. As before, the end of the kinematic phase comes about when the magnetic field is large

enough significantly to alter the driving flow. In this case, however, the new MHD flow is not a statistically marginal dynamo, but rather is incapable of sustaining field against Ohmic diffusion. The field continues to decay until the magnetic energy reaches arbitrarily small values. At this point, the Lorentz force has once again a negligible effect – the velocity is simply responding to the imposed forcing – and we are back in a second kinematic phase. One might therefore expect that we have returned full circle and the *original* kinematic scenario applies so that exponential re-amplification of the field should occur. However, this is not the case, and the magnetic field is never regenerated. This somewhat surprising result can be understood in terms of the hydrodynamic instability of the basic flow U_0 . We have noted in Section 3.3 that the basic flow is unstable, albeit on a slow timescale, to hydrodynamic perturbations. We shall refer to the resulting hydrodynamic flow as U_1 , and note that unlike U_0 it is not time periodic nor maximally helical. For the value of Ω under consideration ($\Omega = 2.5$), this flow is not a kinematic dynamo. Furthermore, the presence of a finite amplitude magnetic field, as the one generated by initial conditions near U_0 , is not enough to prevent a slow relaxation of the system towards $U = U_1$, and $B = 0$. Thus, even though some magnetic field is generated initially by virtue of the somewhat special initial conditions, i.e. $U = U_0$, the system is ultimately not a dynamo.

Some structural differences between the flows U_0 and U_1 can be seen in the volume renderings of enstrophy density shown in Fig. 10(b). These renderings show snapshots in time of the two flows and illustrate that U_1 appears to have a smaller velocity lengthscale whilst retaining traces of the original U_0 structure. The time evolution of the kinetic energy, relative helicity and the velocity lengthscale for the flow U_1 are shown in Fig. 16. These should be contrasted with the corresponding quantities for U_0 that have time-independent values of 1.5, 1.0 and 1.0, respectively. Clearly, U_1 has a more complex temporal behaviour and the reduction in the velocity lengthscale is confirmed. Ideally, one would like to investigate the chaotic properties of U_1 by calculating the Lyapunov exponents as we did for U_0 . However, this is difficult since U_1 does not exist as a simple analytic function and so the exponents would have to be calculated from a numerical integration of the flow.

6.2. Kinematic dynamo properties of the new hydrodynamic state

We now consider the kinematic dynamo properties of the new U_1 flow. These simulations use the same forcing as previously, but this time start with the U_1 solution that remained when the magnetic field had decayed to very low level at $\Omega = 2.5$ as an initial condition instead of the usual ABC flow. Fig. 17 shows that for $\varepsilon = 1$ with initial condition U_1 , the small amount of remaining magnetic field either grows exponentially or continues to decay, depending on the frequency of the forcing Ω . Fig. 18 contrasts the measured kinematic growth rates for dynamo action using U_0 initial conditions (discussed earlier) with those for the U_1 flow. In each case, the imposed forcing functions are identical and it is only the initial hydrodynamic condition that is different. The growth rate of the U_1 flow is again sensitive to Ω but in all cases is lower than the corresponding growth rate for U_0 . The values for U_1 are very small for small Ω , increasing to a maximum value at $\Omega \sim 1$, and decreasing again thereafter. For values of $\Omega \geq 1.7$, the growth rate becomes small and negative for some values. The U_1 flow is in all cases a *worse* kinematic dynamo than the ABC flow, and in some cases not a dynamo at all (as we already saw for $\Omega = 2.5$).

For those values of Ω for which the U_1 flow is a kinematic dynamo (e.g. $\Omega = 1$), the linear phase of growth again saturates when the magnetic energy is large enough to affect the velocity field. In

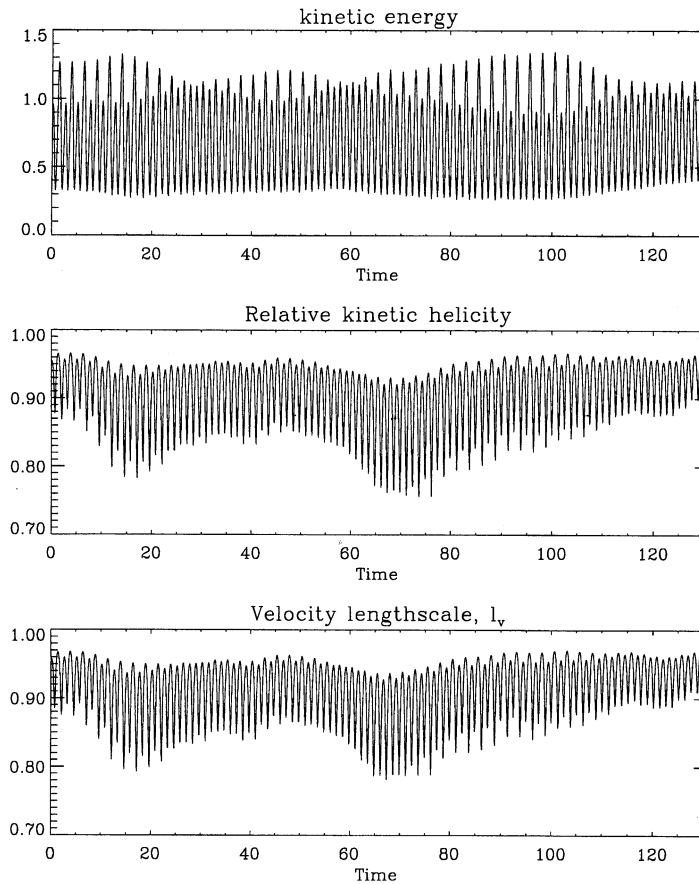


Fig. 16. Kinetic energy (upper panel), relative kinetic helicity (middle panel) and velocity lengthscale (lower panel) as functions of time for the velocity U_1 . Here, $\varepsilon = 1$, $Re = 100$, and $\Omega = 2.5$. In comparison, for U_0 the traces would be steady at 1.5, 1.0 and 1.0, respectively.

this case the field saturates at the same level as for the dynamic saturation of the U_0 initial condition (Fig. 19). Moreover, quantities such as the lengthscale of the magnetic field and of the velocity in the two cases are on average the same. This would seem to imply that, despite the fact that the two flows have different kinematic growth rates and initial conditions, the eventually realised nonlinear MHD state is *the same* in both cases.

The existence, as shown in Fig. 18, of dynamically realisable flows with negligible dynamo growth rate gives rise to interesting nonlinear possibilities. In the kinematic regime, these flows, by virtue of their marginal dynamo properties, leave the magnetic energy unchanged from its initial value. What is remarkable is that this property holds, in so far as it can be verified numerically, even if the initial magnetic field is not infinitesimal. In other words, whatever field energy is present when the velocity relaxes to a U_1 -type flow² will persist forever. Thus, for these flows the long-time behaviour is largely determined by the initial conditions. One can envisage a number of numerical

² A U_1 -type flow is a full MHD flow associated with the hydrodynamic flow U_1 .

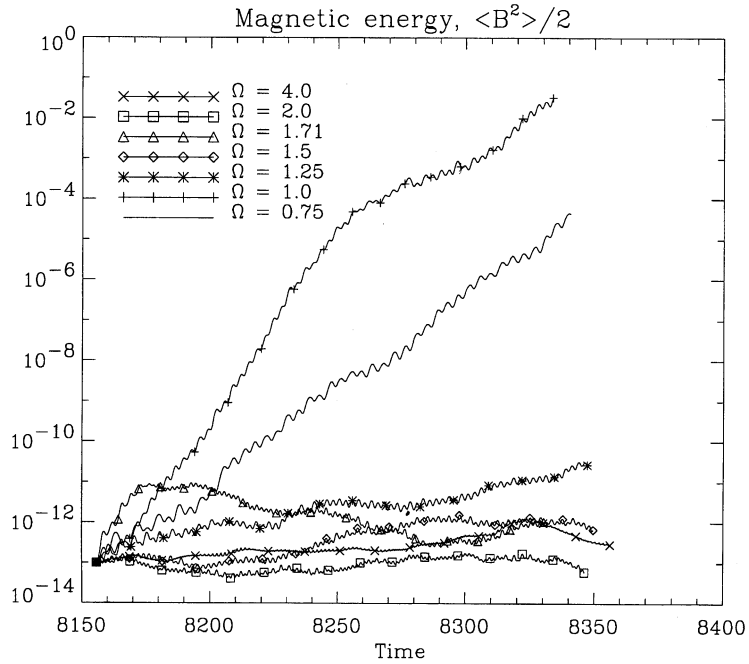


Fig. 17. Magnetic energy growth with time for various Ω , using U_1 as the initial condition. Here $\varepsilon = 1$ and $R_m = Re = 100$.

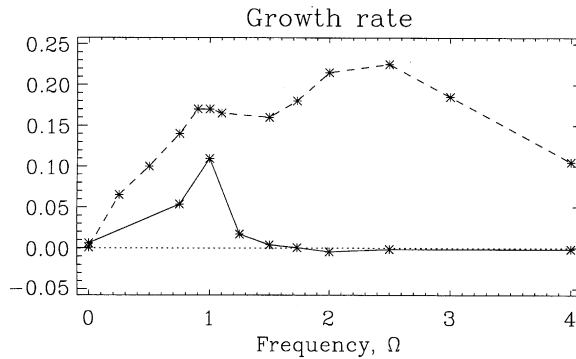


Fig. 18. The variation of the measured kinematic growth rate of the magnetic energy against Ω for the two differing initial conditions, U_1 (—) and U_0 (---), for $\varepsilon = 1$ and $R_m = Re = 100$.

experiments consisting of identical conditions for the velocity, $U(t=0) = U_0$, say, and seed magnetic fields with different amplitudes. All these cases would eventually relax to states where the velocity is of type U_1 , but with different values of the final magnetic energy. The precise values are determined by a combination of the initial magnetic amplitudes and the times to relax the velocity from U_0 to the U_1 -type flows. For initial conditions with efficient kinematic dynamo properties, magnetic field may be amplified so that magnetic perturbations become significant and mediate the transition

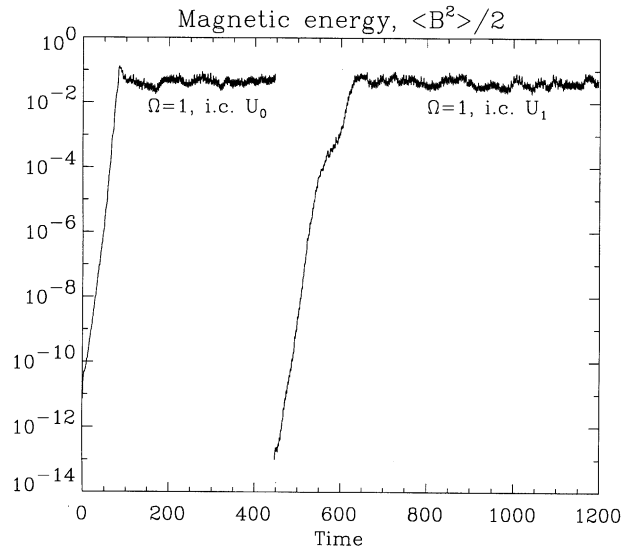


Fig. 19. The saturation of the magnetic energy versus time for two cases which are both kinematic dynamos with the same forcing but which start from different initial conditions, U_0 and U_1 . Here, $\Omega = \varepsilon = 1$ and $R_m = Re = 100$.

to the U_1 -type flow. If the initial conditions are less efficient, then the hydrodynamic instability may engender the U_1 -type flow, and the level of magnetic energy retained by the resulting marginal dynamo depends on that which existed at the time of arrival at that state. Arbitrary levels of magnetic energy could be built in this manner.

7. Conclusions

We have presented the wide range of behaviour of solutions from fully nonlinear forced triply periodic incompressible magnetohydrodynamic simulations in both the kinematic and dynamic (non-linear) regimes. The equations are forced such that, in the absence of magnetic fields, a modified time-dependent ABC flow U_0 results, a flow selected since Lagrangian statistics indicate that it is a good candidate for vigorous kinematic dynamo action.

Fully nonlinear simulations with this forcing, starting from U_0 and a weak state of magnetisation, exhibit a regime where the velocity remains close to U_0 and serves to amplify the magnetic field. A period of exponential growth in the magnetic field can clearly be identified and a growth rate measured. The efficiency of the dynamo action in this kinematic regime depends on the amplitude, ε , and frequency, Ω , of the oscillation involved in the time-dependent forcing. In particular, the growth rate of the kinematic dynamo shows a distinct maximum around $\Omega = 2.5$. The growth rate also depends on the magnetic Reynolds number, R_m , initially increasing, but then saturating to a relatively constant value of the growth rate for $R_m > 50$. The lengthscale of the magnetic field scales as $R_m^{-1/2}$ for all R_m examined here, reflecting a balance of advection and diffusion in the induction equation.

Since these are fully nonlinear calculations, a kinematic amplification of the magnetic field cannot continue indefinitely. Eventually, the magnetic field becomes large enough that the Lorentz force in the momentum equations is significant, and a fully nonlinear MHD state is achieved. We have presented a solution for $\Omega=1$ and $\text{Re}=R_m=100$ which represents the most typical view of nonlinear dynamo action. In this scenario, when the magnetic perturbations become sufficiently large, their effect is to modify the driven velocity via the Lorentz force such that the amplification of the magnetic field is halted and the magnetic energy saturates. The resulting MHD state is stationary and acts as a marginal dynamo, neither amplifying nor destroying magnetic field, so that the finite level of magnetic energy can be sustained for all time. Physically, as the dynamo evolves from the kinematic to the nonlinear regime, the lengthscale of the magnetic field increases, corresponding to a change from the kinematic eigenfunction cigar-like solutions to a state including more sheet-like structure, and the lengthscale of the velocity field decreases, as the driven velocity changes to a more structurally complicated solution.

The scaling of these effects with the parameters has been examined. Despite a jump in value between the kinematic and nonlinear regimes, the magnetic lengthscale continues to scale as $R_m^{-1/2}$, implying that a balance between advection and diffusion in the induction equation is restored, once the equilibration has been effected. The average value of the stationary state magnetic energy in the nonlinear regime eventually saturates as the magnetic Reynolds number gets larger (in a similar manner to the kinematic growth rate), but initially scales like $\text{Re}^{-1}R_m^{1/2}$. This early scaling can be understood in terms of a balance for the magnetically driven part of the velocity between the Lorentz force and viscous diffusion, under certain circumstances. The fact that $B^2 \sim \text{Re}^{-1}$ seems to imply that arbitrarily large saturation magnetic energy can be obtained in the nonlinear regime for small Reynolds numbers, but this is an artifact of the forced equations. The loss of these scalings as R_m is increased indicates that the saturation mechanism becomes independent of diffusion and must be acting in a more subtle manner.

This type of dynamo saturation may be expected to occur wherever kinematic dynamo action is present initially, with differences in the time of arrival at the nonlinear regime and the saturation value, depending on the parameters. However, the solutions for $\Omega = 2.5$ displayed here present an entirely different result. In the kinematic sense, $\Omega = 2.5$ is the best dynamo, since its growth rate is the maximum. However, after the initial kinematic amplification to a large value, the magnetic energy remarkably decays in the nonlinear regime, and does not equilibrate as it did for $\Omega = 1$. The ultimate decay of magnetic field in this way was first studied by Brummell et al. (1998) and can be understood in terms of the stability of the underlying hydrodynamic states. The perturbation provided by the growing magnetic field in this case has driven the resultant MHD state away from one associated with the hydrodynamically unstable initial condition U_0 to one associated with the stable hydrodynamic solution, which we call U_1 . At these parameters, the U_1 -type flow is not a dynamo, and therefore cannot sustain the magnetic field that was created kinematically from the special initial conditions. The U_1 -type MHD state thus decays slowly to reveal the underlying velocity field U_1 .

The dependence of the kinematic growth rate of U_1 on Ω reveals that it is always lower than that for U_0 , indicating that it is a worse kinematic dynamo. Although the flow U_0 may be the convenient choice of solution for a kinematic problem due to its analytic nature and promising Lagrangian properties, the ultimate fate of the nonlinear system is determined by the stable hydrodynamic state U_1 , that possesses less easily defined structure and less efficient kinematic dynamo properties.

Furthermore, for a wide range of Ω ($1.7 < \Omega < 4.0$), the growth rate for U_1 is close to zero. Such flows with *marginal* dynamo properties lead to the intriguing possibility that magnetic field could be maintained at arbitrary values, where the ultimate saturation energy of the field depends upon the initial conditions. For example, for $\Omega \sim 1.7$ the saturation value of the magnetic energy depends upon the kinematic growth rate of the initial hydrodynamic condition and the level of initial weak magnetisation: if the field grows quickly, the magnetic energy may become large and magnetic perturbations via the Lorentz force may equilibrate the system in a U_1 -type flow. Alternatively, if the growth is slow, the flow may evolve to a U_1 -type flow via the hydrodynamic instability at a lower level of the magnetic energy. An example of this two-phase behaviour can be seen in Fig. 5, although at these parameters the U_1 -type flow is a slowly growing kinematic dynamo.

These simulations show (see also Brummell et al., 1998; Fuchs et al., 1999) that different MHD states can exist for a single forcing in the fully nonlinear equations. It may be expected that more states could co-exist at higher Reynolds numbers. The existence of these multiple end-states leads to complications for the definition of dynamo action in the nonlinear regime (Brummell et al., 1998). If one attempted to identify forcings that resulted in dynamo action in the nonlinear regime, paralleling the definitions on velocity fields in kinematic theory, then the classification becomes clouded, since initial conditions must be taken into account. Ultimately, the coexistence of multiple states with different hydrodynamic and hydromagnetic stability properties can yield complicated nonlinear dynamics. Tobias et al. (1995) have further argued that modulation of the solar cycle may arise from such dynamics with trajectories chaotically moving between states leading to intervals of increased and decreased (grand minima) magnetic activity.

One final point regarding the stable hydrodynamic flow U_1 is worthy of mention here, although we leave expansion of this idea to a later date. Taking the U_1 flow at parameters where it is not a kinematic dynamo (e.g. $\varepsilon=1, \Omega=2.5, \text{Re}=100, R_m=100$), and including a small amplitude *mean* (i.e. independent of the horizontal directions) magnetic field results in a measurable α -effect. Remarkably, although the flow cannot generate magnetic field on scales on the order of the periodicity of the domain or smaller, it could act as a dynamo for scales much larger than the velocity lengthscale. The possibility of the existence of such small-scale flows which are large-scale dynamos whilst not amplifying field on the small scale is intriguing.

In summary, we have presented results which exhibit the range of subtle behaviour that nonlinear systems can engender. We conclude that the nonlinear aspects of dynamo action are complicated, and seeking a relationship between the kinematic and dynamic regimes is difficult. It is of great interest to extend these ideas to more general types of forcing.

Acknowledgements

We would like to thank David Hughes and Nigel Weiss for useful scientific discussions. This work was supported in part by the NASA HPCC program at the Universities of Colorado and Chicago (NASA Grant NCCS1-157), and the NASA SR&T program through Grant NAG5-4953. We would also like to thank the computing staff at the Cornell Theory Center, where the simulations were carried out on the IBM SP2.

References

- Arnol'd, V.I., Korkina, E.I., 1983. The growth of a magnetic field in a three-dimensional steady incompressible flow. *Vest. Mosk. Un. Ta. Ser. 1, Matem. Mekh.* 3, 43–46.
- Brummell, N.H., Cattaneo, F., Tobias, S.M., 1998. Linear and nonlinear dynamo action. *Phys. Lett. A* 249, 437–442.
- Canuto, C., Hussaini, M.Y., Quarteroni, A., Zang, T.A., 1988. *Spectral Methods in Fluid Dynamics*. Springer, Berlin.
- Cattaneo, F., 1999. On the origin of magnetic fields in the quiet photosphere. *Astrophys. J. Lett.* 515, 39–42.
- Cattaneo, F., Hughes, D.W., Kim, E., 1996. Suppression of chaos in a simplified nonlinear dynamo model. *Phys. Rev. Lett.* 76, 2057–2060.
- Cattaneo, F., Kim, E., Proctor, M.R.E., Tao, L., 1995. Fluctuations in quasi-two-dimensional fast dynamos. *Phys. Rev. Lett.* 75, 1522–1525.
- Childress, S., Gilbert, A.D., 1995. *Stretch, Twist, Fold: The Fast Dynamo*. Springer, Berlin.
- Cowling, T.C., 1957. *Magnetohydrodynamics*. Interscience, New York.
- Dombre, T., Frisch, U., Greene, J.M., Hénon, M., Mehr, A., Soward, A.M., 1986. Chaotic streamlines in the ABC flows. *J. Fluid Mech.* 167, 353–391.
- Fuchs, H., Rädler, K.-H., Rheinhardt, M., 1999. On self-killing and self-creating dynamos. *Astron. Nachr.* 320, 129–133.
- Galanti, B., Pouquet, A., Sulem, P.L., 1993. Influence of the period of an ABC flow on its dynamo action. In: Proctor, M.R.E., Matthews, P.C., Rucklidge, A.M. (Eds.), *Solar and Planetary Dynamos*, Publications of the Newton Institute, Vol. 1. Cambridge University Press, Cambridge, pp. 99–103.
- Galanti, B., Sulem, P.L., Pouquet, A., 1992. Linear and non-linear dynamos associated with ABC flows. *Geophys. Astrophys. Fluid Dyn.* 66, 183–208.
- Galloway, D.J., Frisch, U., 1984. A numerical investigation of magnetic field generation in a flows with chaotic streamlines. *Geophys. Astrophys. Fluid Dyn.* 29, 13–18.
- Galloway, D.J., Frisch, U., 1986. Dynamo action in a family of flows with chaotic streamlines. *Geophys. Astrophys. Fluid Dyn.* 36, 53–83.
- Galloway, D.J., O'Brian, N.R., 1993. Numerical calculations of dynamos for ABC and related flows. In: Proctor, M.R.E., Matthews, P.C., Rucklidge, A.M. (Eds.), *Solar and Planetary Dynamos*. Publications of the Newton Institute, Vol. 1. Cambridge University Press, Cambridge, pp. 105–113.
- Galloway, D.J., Proctor, M.R.E., 1992. Numerical calculations of fast dynamos in smooth velocity fields with realistic diffusion. *Nature* 356, 691–693.
- Galloway, D.J., Proctor, M.R.E., Weiss, N.O., 1978. Magnetic flux ropes and convection. *J. Fluid Mech.* 87, 243–261.
- Kida, S., Yanase, S., Mizushima, J., 1991. Statistical properties of MHD turbulence and turbulent dynamo. *Phys. Fluids A* 3, 457–465.
- Lau, Y.-T., Finn, J.M., 1993. Fast dynamos with finite resistivity in steady flows with stagnation points. *Phys. Fluids B* 5, 365–375.
- Meneguzzi, M., Pouquet, A., 1989. Turbulent dynamos driven by convection. *J. Fluid Mech.* 205, 297–318.
- Moffatt, H.K., 1972. An approach to a dynamic theory of dynamo action in a rotating conducting fluid. *J. Fluid Mech.* 53, 385–399.
- Moffatt, H.K., 1978. *Magnetic Field Generation in Electrically Conducting Fluids*. Cambridge University Press, Cambridge.
- Nordlund, Å., Brandenburg, A., Jennings, R.L., Rieutord, M., Ruokolainen, J., Stein, R.F., Tuominen, I., 1992. Dynamo action in stratified convection with overshoot. *Astrophys. J.* 392, 647–652.
- Parker, E.N., 1979. *Cosmical Magnetic Fields*. Clarendon Press, Oxford.
- Podvigina, O.M., 1999. Spatially-periodic steady solutions to the three-dimensional Navier-Stokes equation with the ABC-force. *Physica D* 128, 250–272.
- Podvigina, O.M., Pouquet, A., 1994. On the nonlinear stability of the 1/1/1 ABC flow. *Physica D* 75, 471–508.
- Ponty, Y., Pouquet, A., Rom-Kedar, V., Sulem, P.L., 1993. Dynamo action in a nearly integrable chaotic flow. In: Proctor, M.R.E., Matthews, P.C., Rucklidge, A.M. (Eds.), *Solar and Planetary Dynamos*. Publications of the Newton Institute, Vol. 1. Cambridge University Press, Cambridge, pp. 241–248.
- Ponty, Y., Pouquet, A., Sulem, P.L., 1995. Dynamos in weakly chaotic 2-dimensional flows. *Geophys. Astrophys. Fluid Dyn.* 79, 239–257.
- Seehafer, N., Feudel, F., Schmidtman, O., 1996. Nonlinear dynamo with ABC forcing. *Astron. Astrophys.* 314, 693–699.

- Soward, A.M., 1994. Fast Dynamos. In: Proctor, M.R.E., Gilbert, A.D. (Eds.), *Lectures on Solar and Planetary Dynamos*. Publications of the Newton Institute, Vol. 2. Cambridge University Press, Cambridge, pp. 181–217.
- Tobias, S.M., Weiss, N.O., Kirk, V., 1995. Chaotically modulated stellar dynamos. *Mon. Not. Roy. Astron. Soc.* 273, 1150–1166.
- Zel'dovich, YA.B., Ruzmaikin, A.A., Sokoloff, D.D., 1983. *Magnetic Fields in Astrophysics*. Gordon & Breach Science Publishers, London.
- Zheligovsky, O., Pouquet, A., 1993. Hydrodynamic stability of the ABC flow. In: Proctor, M.R.E., Matthews, P.C., Rucklidge, A.M. (Eds.), *Solar and Planetary Dynamos*. Publications of the Newton Institute, vol. 1. Cambridge University Press, Cambridge.
- Zienicke, E., Politano, H., Pouquet, A., 1998. Variable intensity of lagrangian chaos in the nonlinear dynamo problem. *Phys. Rev. Lett.* 81, 4640–4640.